

# Dimensional Changes During Solvent-Induced Crystallization of Poly(ethylene Terephthalate) Films

CHRISTOPHER J. DURNING\* and LUDWIG REBENFELD, *Textile Research Institute and Department of Chemical Engineering, Princeton University, Princeton, New Jersey 08540*

## Synopsis

The sample dimensional changes accompanying diffusion with induced crystallization in amorphous poly(ethylene terephthalate) (PET) films are analyzed. Initially, the film's lateral area remains practically constant, but near the end of the process, it increases rapidly, consistent with non-Fickian models for diffusion. The ultimate relative thickness increase is about double that for the lateral dimension, implying that plastic deformation in the thickness direction accompanies the sorption. Plots of fractional area increase ( $\Delta A/\Delta A_\infty$ ) vs. fractional weight gain ( $W/W_\infty$ ) indicate severe softening of the polymer by the penetrant.

## INTRODUCTION

Recent research in this laboratory has produced poly (ethylene terephthalate) (PET) fibers with a unique "bimorphic" morphology; extremely porous surface material overlays a strain hardened core.<sup>1</sup> Such materials may be of interest in applications where surface properties dictate performance, as in filtration or in composites. Bimorphic fibers result from briefly contacting amorphous, unoriented filaments with interactive organic liquids, i.e., penetrants which depress the glass transition temperature of the polymer below the environmental temperature. As a result of the simultaneous sorption and crystallization during contact, extreme surface porosity may develop, but the exact surface morphology depends critically on the contacting conditions.<sup>2,3</sup> The present investigations<sup>2-5</sup> of solvent-induced crystallization (SINC) in PET are aimed at developing an accurate description of the process to allow intelligent manipulation of the fiber contacting conditions. Companion publications report on the mathematical modeling of the process<sup>4</sup> and on the sorption kinetics.<sup>5</sup>

The sorption of interactive penetrants during SINC is currently thought to be Fickian<sup>6,7</sup>; however, the observations of moving boundaries in these systems<sup>8</sup> suggests the process is non-Fickian by analogy with transport processes in noncrystallizable, glassy polymers.<sup>9</sup> Sample dimensional changes accompanying organic vapor sorption can clearly detect non-Fickian transport when present.<sup>10-15</sup> It is therefore reasonable to examine sample

\* Current address: Department of Chemical Engineering and Applied Chemistry, Columbia University, New York, NY 10027.

dimensional changes during SINC in order to clarify the diffusion mechanism.

To provide a basis for subsequent discussion, we review briefly some of the previous treatments of sample dimensional changes during non-Fickian diffusion. Park<sup>10</sup> measured the lateral area of polystyrene sheets during the sorption of methylene chloride (MeCl) vapor, noting a very slow increase during most of the sorption process but a rapid rise near the end, indicating a constraint to the isotropic expansion of the sheet which is relieved when the film is practically saturated. Drechsel et al.<sup>12</sup> studied the sorption of acetone vapor in cellulose nitrate films cast from solution on mercury. This system also shows lateral area increases delayed until near the end of sorption. However, sorption-desorption cycles progressively reduced the lateral area of the dry films and concomitantly increased their thickness. The resulting films showed molecular orientation normal to the plane of the film. Apparently the constrained expansion during sorption produced chain alignment in the diffusion direction in this system.

Crank<sup>11</sup> first modeled the non-Fickian diffusion process using a strain dependent diffusion coefficient ( $D$ ), which also increased stepwise at a critical concentration, predicting two distinct regions of the sample during sorption: a swollen outer layer whose thickness increases progressively and a dry, glassy core whose thickness decreases progressively. Crank assumed both layers to be elastic with different moduli. The expansion of the film's lateral area results from the balance of compressive forces exerted by the core on the swollen layer against tensile forces exerted by the swollen layer on the core. Since the modulus of the core is much larger than that of the swollen layer, the model predicts almost no lateral expansion until the core has very small dimensions, as it does near the end of sorption.

Petropoulos and Roussis<sup>13</sup> improved Crank's model by using a stress-dependent diffusion coefficient (rather than a strain-dependent one) which increases exponentially with concentration. They also considered linear viscoelastic mechanical behavior of the polymer (the mechanical equivalent of a spring in parallel with a Maxwell element) with the mechanical constants decreasing exponentially with concentration. When the fractional area increase,  $\Delta A/\Delta A_\infty$ , is plotted against the fractional weight gain,  $W/W_\infty$ , curves characteristic of the model's mechanical constants result. For perfectly elastic media (i.e., setting the viscosity to zero or infinity) with a concentration independent modulus,  $\Delta A/\Delta A_\infty$  equals  $W/W_\infty$  throughout sorption. However, if the modulus decreases significantly with concentration (an effect called "softening" in Ref. 13), and/or the material is viscoelastic with a characteristic relaxation time comparable to the characteristic diffusion time, then  $\Delta A/\Delta A_\infty$  deviates below  $W/W_\infty$  during sorption. For viscoelastic behavior, the extent of the deviations depend on the film thickness;  $\Delta A/\Delta A_\infty$  falls further below  $W/W_\infty$  in thicker films.

Recently, Thomas and Windle<sup>14,15</sup> measured simultaneously the thickness and lateral area changes during the sorption of methanol in thin poly(methyl methacrylate) (PMMA) sheets from room temperature to 60°C; Figure 1 shows schematically the sequence of dimensional changes they found. As in the systems discussed above, the films swelled anisotropically (in the thickness direction only) before complete penetration by the solvent

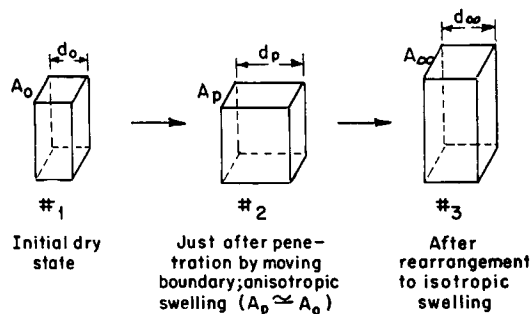


Fig. 1. Schematic representation of dimensional changes during non-Fickian diffusion of solvents in glassy polymer sheets.

owing to the lateral constraint of the glassy core. In the case of PMMA and methanol, after complete penetration the samples rearranged spontaneously to an isotropically swelled state, regaining their original relative dimensions. Interestingly, however, even when the advancing concentration profiles were steplike (i.e., without gradients behind the moving boundary), the removal of the glassy core increased the solubility of the diluent in the polymer. For steplike profiles Thomas and Windle related the solubility in the anisotropically swelled state (#2 in Fig. 1) to that in the isotropically swelled state (#3 in Fig. 1) by combining the Wall theory of rubber elasticity with the Flory-Huggins equation for the free energy of mixing. By assuming that the polymer molecules assume more or less random coil configurations in the dry state and that the physical network points remain intact during both sorption and rearrangement from anisotropic to isotropic states, Thomas and Windle derived

$$\frac{\ln(1 - \phi) + \phi + \chi\phi^2}{\phi^{1/3} - \phi} = \frac{\ln(1 - \phi_p) + \phi_p + \chi\phi_p^2}{1/\phi_p - \phi_p} \quad (1)$$

where  $\phi_p$  is the polymer volume fraction in the anisotropic state,  $\phi$  is the polymer volume fraction in the isotropic state, and  $\chi$  is the interaction parameter. The volume fractions  $\phi_p$  and  $\phi$  can be calculated directly from the dimensional changes with respect to the dry sample (#1 in Fig. 1), assuming additivity of polymer and solvent volumes.

## EXPERIMENTAL

### Materials

Dr. C. Heffelfinger (E. I. duPont de Nemours and Co.) supplied unoriented, amorphous PET films. Two film thicknesses were used:  $0.030 \pm .0003$  cm (12 mil) and  $0.086 \pm .008$  cm (33.8 mil). Wide angle X-ray scattering (courtesy of Dr. H. D. Noether) verified the amorphous nature of the films. Elemental analysis by X-ray fluorescence spectroscopy (courtesy of Dr. Noether) showed minor levels of typical additives ( $\text{TiO}_2$ , Ca, P). Differential scanning calorimetry using a heating rate of  $20^\circ\text{C}/\text{min}$  gave a glass transition temperature of  $76^\circ\text{C}$  for both films. To prevent slow structural de-

velopment, the samples were kept frozen until ready for use, when they were conditioned for 12 h at 70°F and 65% RH. Reagent grade methylene chloride (MeC1) and dimethylformamide (DMF) were used for the sorption experiments.

### Dimensional Measurements

Two procedures were employed to determine the dimensional changes of conditioned samples during vapor sorption. In the first, samples were suspended above liquid solvent in an enclosed, thermostatted ( $\pm 0.5^\circ\text{C}$ ) cell. Periodic agitation of the liquid assured a uniform vapor concentration within the cell. After exposure for a certain period, sample thickness and area were measured with a preloaded micrometer and a traveling microscope, respectively. A fresh sample was used for each exposure time and separate sets of experiments for thickness, and area measurements minimized volatilization time of the penetrant after removal of the specimen from the solvent cell. In a second procedure the dimensional changes in a sample were monitored *in situ*. Separate samples were used for thickness and lateral area changes. The specimens were mounted vertically or horizontally on a wire frame enclosed in a glass cell containing the liquid solvent. With the cell positioned on a microscope stage (Leitz Inc. "Ortholux"), the sample dimensions were measured with a filar micrometer eye piece.

The time required for complete penetration of the film by the solvent front was also determined. In moderately thick, amorphous PET films ( $>0.01$  cm thick) exposed to interactive vapors, crystallization occurs immediately behind the solvent front.<sup>8</sup> Since the transparent core could be clearly observed with either microscope by illuminating the sample from below, the time when the transparent core disappeared was taken as the penetration time.

### Sorption Measurements

We measured the weight gain kinetics of MeC1 and DMF vapors in conditioned samples using a deflection spring balance described in detail elsewhere.<sup>5</sup> A sample was suspended by a fine wire just above the liquid solvent in an enclosed thermostatted cell ( $\pm 0.5^\circ\text{C}$ ). The wire was connected to a phosphor-bronze wire helix above the cell through a 1mm bore perforation. A linear variable differential transformer (Schaevitz) monitored the deflection of the helix. The liquid in the cell was agitated continuously to ensure a uniform vapor concentration within the cell.

### Density Measurements

The densities of amorphous and solvent crystallized samples were determined by the density gradient technique (ASTM #D1505) using inert liquid media (*n*-heptane and carbon tetrachloride). Sample positions were read with a sensitive cathetometer after 72 h of settling time, and the apparent densities were calculated by linear interpolation between the positions of calibrated glass floats.

In the case of solvent crystallized films, the void formation during crys-

tallization and the entrapment of solvent in the crystalline structure can affect the specimen's apparent density<sup>16-19</sup>; we employed crystallization conditions and solvent removal procedure which minimize these effects.

Two types of void structures can result from solvent induced crystallization: macrovoids with characteristic dimensions of 1–5  $\mu\text{m}$  and microvoids with dimensions of 10–20  $\text{\AA}$ , both of which have been avoided in this work. Scanning electron microscopy<sup>2,20</sup> showed clearly that saturated MeCl and DMF vapors do not induce macrovoid development in initially amorphous PET films. Further, Weigmann et al.<sup>17,18</sup> and Jameel et al.<sup>21</sup> found previously that very little microvoid development resulted from solvent modification of PET at temperatures below 100°C, particularly if the crystallizing solvent was removed gradually from the swollen structure. Therefore, to minimize the microvoid development in our samples, the solvent crystallized films were air-dried at room temperature for 24 h and subsequently dried under a moderate vacuum (0.02 Torr) for 24 h.

Unavoidably, a very small amount of solvent (1–2 wt %) became trapped within the crystalline structure. For each sample, the amount of residual solvent was determined by weighing and the actual polymer density was deduced from the residual content and the measured apparent density following Sheldon.<sup>19</sup>

The polymer densities determined by our procedure give very reasonable estimates for the ultimate volume fraction crystallized during solvent exposure (30–40% using the constants published by Kilian<sup>22</sup>).

## RESULTS AND DISCUSSION

Figures 2–4 summarize the dimensional changes recorded. Figures 2 and 4 show data gathered using the first procedure, while Figure 3 shows data using the second. For the former cases, the data scatter arise from the variation in initial film thicknesses among the specimens, so an average film thickness was used in the calculation of relative thickness changes, which confines the scatter to the portion of the curve following complete penetration.

The data typify non-Fickian diffusion; because of a rigid core, the sample swells almost entirely in the thickness direction until near the end of the sorption process. The vertical dashed lines in Figures 2–4 demark the estimates for the time of complete saturation, which roughly precedes the rapid increases in lateral area. These estimates correspond to the time when a sudden decrease in the rate of weight uptake occurs, near the end of sorption.<sup>5</sup> Note that the thickness does not drop significantly during the increase in lateral area (i.e.,  $d_p \cong d_\infty$  in Fig. 1), contrary to the result found for methanol in PMMA.<sup>15</sup>

The extent to which the sorption process alters the relative dimensions of the sample can be calculated. This shows whether sorption causes any permanent distortion of the sample. If the sample retains its original proportions, the relative thickness and area changes are related by

$$\frac{\Delta A_\infty}{A_0} = \left(\frac{\Delta d_\infty}{d_0}\right)^2 + \frac{2\Delta d_\infty}{d_0} \quad (2)$$

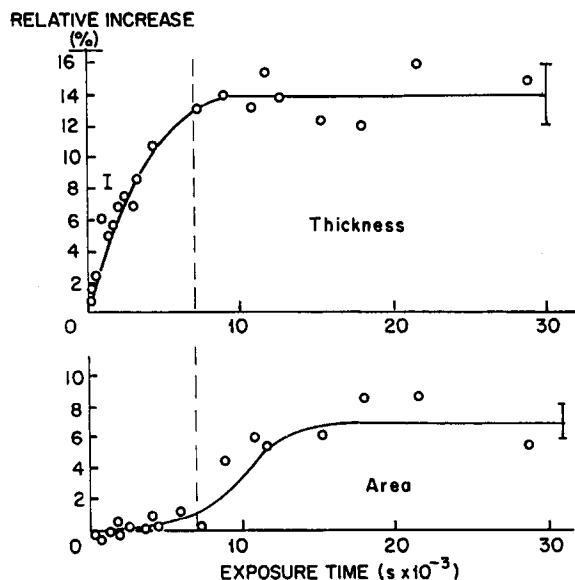


Fig. 2. Dimensional changes in 0.086 cm (33.8 mil) PET film during the sorption of saturated MeCl vapor at 38°C.

where  $\Delta A_{\infty}/A_0$  and  $\Delta d_{\infty}/d_0$  are the final relative area and thickness changes, respectively. Table I compares the left and right hand sides of eq. (2), using the data in Figures 2-4. Table I shows the films do not retain their original dimensional proportions after sorption. The ratio  $c_2/c_1$  indicates that the relative thickness increase is about twice the relative increase in the lateral dimension. This result implies that sorption causes plastic deformation in the thickness direction which supports the ductile deformation mechanism for non-Fickian diffusion in PET proposed else-

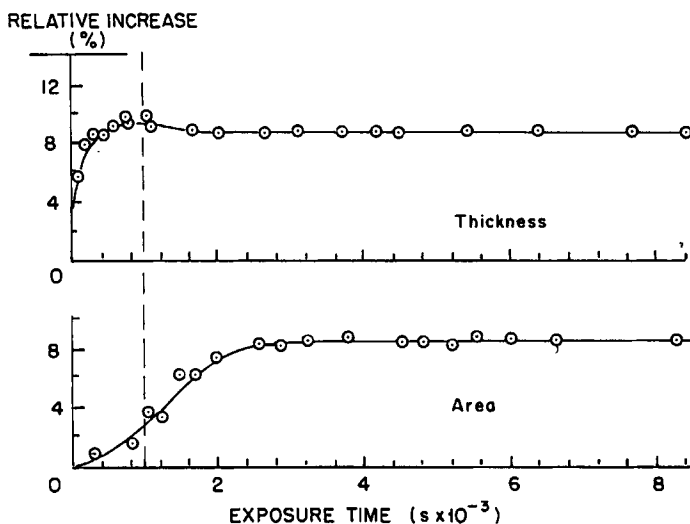


Fig. 3. Dimensional changes in 0.03 cm (12 mil) PET film during the sorption of saturated MeCl vapor at 22°C.

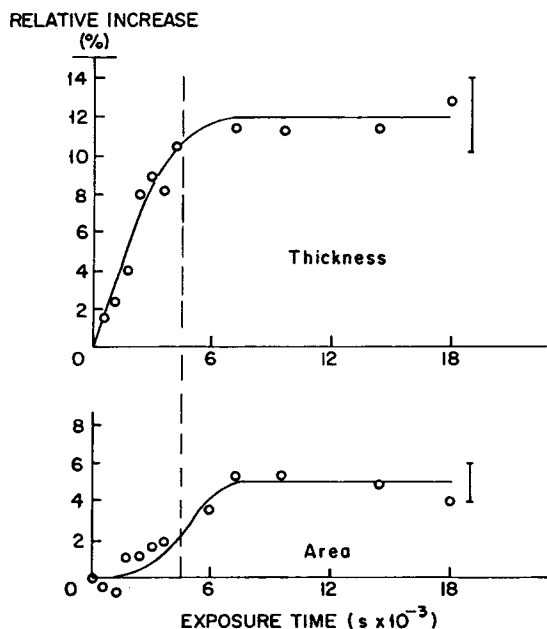


Fig. 4. Dimensional changes in 0.03 cm (12 mil) PET film during the sorption of saturated DMF vapor at 55°C.

where.<sup>5</sup> Although no direct measurements were made, we do not believe that repeated sorption/desorption cycles would further distend the specimen's thickness as found for acetone in cellulose nitrate<sup>12</sup> since the crystallinity induced during the first sorption produces a physical network which would resist further plastic deformation. This idea seems reasonable since the sorption kinetics measured during second and third resorptions were found to be identical.<sup>20</sup>

Plotting the fractional area increase,  $\Delta A/\Delta A_\infty$ , against the fractional weight gain,  $W/W_\infty$ , during sorption results in curves characteristic of the material's mechanical response to swelling stresses. Such plots appear in Figures 5-7. In each case  $\Delta A/\Delta A_\infty$  falls below  $W/W_\infty$  throughout sorption, indicating that the polymer "softens" as described earlier and/or the system behaves viscoelastically with a characteristic response time comparable to the characteristic diffusion time. We cannot discriminate between these effects with the data presented here, although considerable softening in the sense discussed in Ref. 13 is certainly to be expected in view of the drastic depression of the PET's glass transition temperature by interactive penetrants.<sup>2,8</sup> Additional data such as those in Figures 5-7 using a systematic

TABLE I  
Ultimate Relative Dimensional Changes

Figure	$\Delta A_\infty/A_0 = c_1$	$\Delta d_\infty/d_0$	$(\Delta d_\infty/d_0)^2 + 2\Delta d_\infty/d_0 = c_2$	$c_2/c_1$
2	$0.07 \pm 0.02$	$0.14 \pm 0.02$	$0.30 \pm 0.05$	$2.1 \pm 0.5$
3	$0.086 \pm 0.002$	$0.089 \pm 0.002$	$0.186 \pm 0.004$	$1.47 \pm 0.09$
4	$0.05 \pm 0.01$	$0.12 \pm 0.01$	$0.26 \pm 0.02$	$2.3 \pm 0.3$

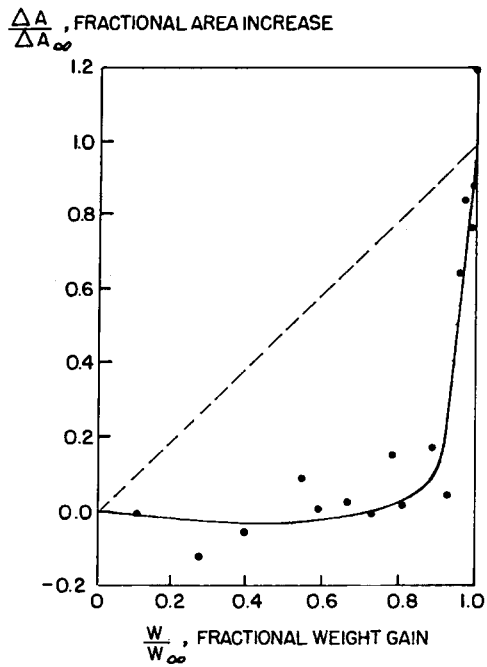


Fig. 5. Fractional area increase vs. fractional weight gain for the conditions in Figure 2.

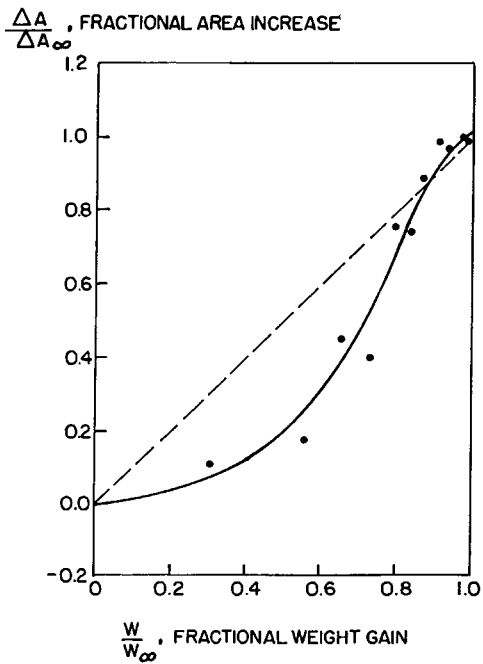


Fig. 6. Fractional area increase vs. fractional weight gain for the conditions in Figure 3.



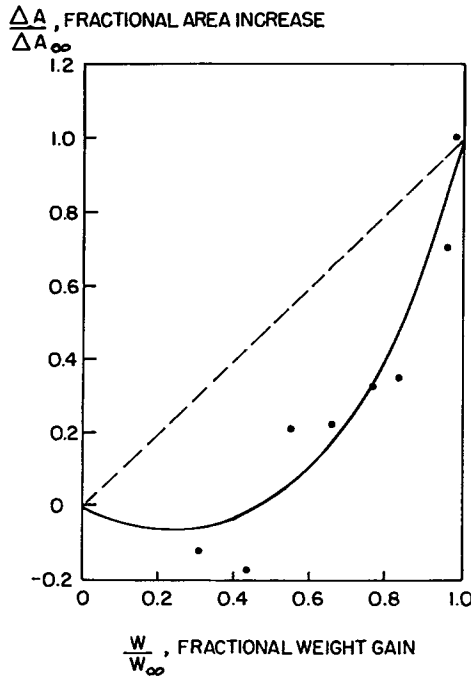


Fig. 7. Fractional area increase vs. fractional weight gain for the conditions in Figure 4.

variation in film thickness might help resolve the role of viscoelasticity in this sorption process.<sup>13</sup>

We have also attempted the calculation of the Flory-Huggins parameter from the dimensional changes, using eq. (1). Here we assume that the Wall theory models adequately the swollen, semicrystalline polymer. Recall that two conditions must be satisfied to apply eq. (1): the concentration profiles during sorption are steplike, and the network structure of the polymer remains intact from states #1-#3 in Figure 1. The mathematical modeling of sorption in the systems studied here<sup>4</sup> suggests strongly that the concentration profiles are essentially steplike, with rather shallow gradients in the swollen portion of the sample. However, the plastic deformations discussed earlier indicate that some change in the system's effective network structure takes place during sorption. We cannot assess quantitatively the error committed by ignoring this effect, and therefore one should not consider the value of  $\chi$  calculated by this method to be definitive.

In terms of the dimensional changes, the final polymer volume fraction in eq. (1) is

$$\phi = \frac{\rho_a A_0 d_0}{\rho_c A_\infty d_\infty} = \frac{\rho_a/\rho_c}{(1 + \Delta A_\infty/A_0)(1 + \Delta d_\infty/d_0)} \quad (3)$$

where  $\rho_a$  and  $\rho_c$  are the densities of the amorphous and semicrystalline polymer, respectively, and the remaining symbols are defined in Figure 1. The ratio  $\rho_a/\rho_c$  accounts for the change in the polymer specific volume

during sorption owing to solvent-induced crystallization. The polymer volume fraction just after penetration is

$$\phi_p = \frac{\rho_a d_0}{\rho_c d_p} = \frac{\rho_a/\rho_c}{(1 + \Delta d_p/d_0)} \quad (4)$$

Given values of  $\phi$  and  $\phi_p$ , a unique value of  $\chi$  follows from eq. (1). The scatter in the sample's final dimensions in Figures 2 and 4 led to unacceptable uncertainties in  $\chi$ , but acceptable accuracy was achieved using the data from Figure 3; these give  $\chi = 1.01 \pm .08$  for MeCl in PET at 22°C.

## CONCLUSIONS

The kinetics of sample dimensional changes for amorphous PET exposed to MeCl and DMF vapors showed characteristics typical of non-Fickian diffusion; during most of the sorption process, the films swelled predominantly in the thickness direction with the lateral area increasing rapidly only near the end of sorption. Non-Fickian transport models explain this sequence; an inner, dry core constrains the film's lateral expansion until after complete penetration by steep solvent profiles. An independent determination of the time for the core's disappearance in our system supports this description.

The measurements showed that sorption changes the samples dimensional proportions. In particular, a permanent distension in the thickness direction results. This suggests that sorption causes plastic deformation supporting the hypothesis of a ductile deformation mechanism for non-Fickian diffusion in amorphous PET given elsewhere.<sup>5</sup>

Plots of the film's fractional area increase vs. the fractional weight gain implied considerable softening of the polymer by penetrant. The possible role of a viscoelastic material response to swelling stresses could not be assessed with the data presented.

The authors thank Professor W. B. Russel and Dr. H.-D. Weigmann for helpful discussions. Ms. Sigrid Ruetsch assisted in the experimental setup. Financial support from the National Science Foundation (DMR-7905980) is gratefully acknowledged.

## References

1. E. A. Gerold, L. Rebenfeld, M. G. Scott, and H.-D. Weigmann, *Text. Res. J.*, **49**, 652 (1979).
2. C. J. Durning, M. G. Scott, and H.-D. Weigmann, *J. Appl. Polym. Sci.*, **27**, 3597 (1982).
3. A. Gozdz and H.-D. Weigmann, *Text. Res. J.*, to appear.
4. C. J. Durning and W. B. Russel, *Polymer*, to appear.
5. C. J. Durning, W. B. Russel, and L. Rebenfeld, to appear.
6. A. B. Desai and G. L. Wilkes, *J. Polym. Sci. Symp.*, **46**, 291 (1974).
7. P. J. Makarewicz and G. L. Wilkes, *J. Polym. Sci., Polym. Phys. Ed.*, **16**, 1529 (1979).
8. P. J. Makarewicz and G. L. Wilkes, *J. Polym. Sci., Polym. Phys. Ed.*, **16**, 1559 (1979).
9. T. Alfrey, Jr., E. F. Gurnee, and W. O. Lloyd, *J. Polym. Sci., C*, **12**, 249 (1966).
10. G. S. Park, *J. Polym. Sci.*, **11**, 97 (1953).
11. J. Crank, *J. Polym. Sci.*, **11**, 151 (1953).
12. P. Drechsel, J. L. Hoard, and F. A. Long, *J. Polym. Sci.*, **10**, 241 (1952).
13. J. H. Petropoulos and P. P. Roussis, *J. Membr. Sci.*, **3**, 343 (1978).

14. N. L. Thomas and A. H. Windle, *J. Membr. Sci.*, **3**, 337 (1978).
15. N. L. Thomas and A. H. Windle, *Polymer*, **22**, 627 (1981).
16. E. L. Lawton and D. M. Cates, *Text. Res. J.*, **48**, 478 (1978).
17. H.-D. Weigmann, M. G. Scott, A. S. Ribnick, and L. Rebenfeld, *Text. Res. J.*, **46**, 574 (1976).
18. H.-D. Weigmann, M. G. Scott, and A. S. Ribnick, *Text. Res. J.*, **47**, 761 (1977).
19. W. R. Moore and R. P. Sheldon, *Polymer*, **2**, 315 (1961).
20. C. J. Durning, Ph. D. thesis, Department of Chemical Engineering, Princeton University, 1983.
21. H. Jameel, H. D. Noether, and L. Rebenfeld, *J. Appl. Polym. Sci.*, **27**, 773 (1982).
22. H. G. Kilian, *Kolloid Z.*, **176**, 49 (1961).

Received August 19, 1983

Accepted February 13, 1984